Coexistence of spin-Peierls and antiferromagnetic Néel states in doped $CuGeO_3$: A magnetic-phase-diagram approach

P. Fronzes and M. Poirier
Centre de Recherche en Physique du Solide, Département de Physique, Université de Sherbrooke, Québec, Canada J1K 2R1

A. Revcolevschi and G. Dhalenne
Laboratoire de Chimie des Solides, Université Paris-Sud, 91405 Orsay Cédex, France
(Received 15 October 1996)

The magnetic-phase diagram of $Cu_{1-x}Zn_xGeO_3$ crystals is obtained with an ultrasonic velocity measurement. As the concentration x is increased both a limited spin-Peierls (SP) order and an antiferromagnetic (AF) order are observed. The AF state is identified through an additional elastic anomaly: its symmetry is orthorhombic with the easy axis along the chain direction. The SP state is clearly identified via a well-defined anomaly at low concentrations only: it is, however, revealed by pretransitional elastic fluctuations for all crystals. From the general aspect of the magnetic phase diagram, we establish that there is coexistence of the SP and AF order at low temperatures. [S0163-1829(97)01414-8]

I. INTRODUCTION

Many theoretical and experimental studies have recently been devoted to the first inorganic spin-Peierls (SP) compound $CuGeO_3$. The coexistence of the SP state and long-range antiferromagnetic order (AF) in Zn (Refs. 1–6) and Si (Refs. 7–9) doped crystals has, in particular, attracted a lot of attention since it was concluded theoretically that this cannot occur at the same time in a unique phase.[10] Evidence for the coexistence of the lattice dimerization and the AF order has however been revealed by neutron-diffraction experiments: both superlattice peaks and magnetic Bragg peaks are observed below the Néel temperature (T_N) in $Cu_{1-x}Zn_xGeO_3$ with $x=0.02$–0.06 (Ref. 4) and in $CuGe_{1-x}Si_xO_3$ with $x=0.007$ (Ref. 9). Very recently it has been showed theoretically with a phase Hamiltonian technique[11] that a disorder-induced AF order is possible in the SP system $CuGeO_3$ doped with Si and Zn. Following this approach the average magnetic moment on the Cu sites is reduced, a result which is consistent with the neutron-diffraction study of Hase *et al.*[3]

The investigation of the magnetic phase diagram of doped SP crystals can help to determine the effect of doping on the magnetic interactions and to understand the competition between the SP and AF Néel states. It has been argued,[12] for example, that enhanced limitation of the SP order is found in the Si compounds due probably to strong structural disorder caused by the strain field of the substituent. It is thus important to observe the effects of this structural disorder on the magnetic phase diagram and to evaluate the differences between Si- and Zn-doped crystals. At present, there seems to be a significant difference in the magnetic excitations between the Zn-doped and Si-doped $CuGeO_3$, although these two systems have many common magnetic properties. This has been shown recently by Hase *et al.*[13] using electron spin resonance (ESR) where AF spin-wave excitations were observed at the magnetic-zone center. We reported recently[8] the doping effects on the magnetic phase diagram of $CuGe_{1-x}Si_xO_3$ with $x=0.007$ and 0.01. The diagram was similar to the one obtained for pure SP compounds: it contained additional AF states below 4 K, among which a spin-flop (SF) phase for the magnetic field oriented along the chain axis, but a coexistence of SP and AF states could not be established.

We report in this paper the magnetic phase diagram of $Cu_{1-x}Zn_xGeO_3$ single crystals with x covering the useful concentration range. The diagrams are obtained by investigating the elastic anomalies in the ultrasonic velocity occurring at the magnetic-phase transitions. Our results confirm that the structural disorder is less severe in Zn-doped crystals and that an AF Néel state with orthorhombic anisotropy is established and coexists with a limited SP state.

II. EXPERIMENT

The $Cu_{1-x}Zn_xGeO_3$ single crystals with $x=0$, 0.006, 0.015, 0.032 and >0.05 were grown from the melt by a floating zone method associated to an image furnace.[14,15] The determination of the Zn content was made by inductively coupled plasma atomic emission spectrometry (ICP/AES).[16] The crystal shape is a cylinder several cm long with an elliptical cross section. Since the crystals cleaved readily along the (100) plane, the orthorhombic axes b and c are easily identified to the minor and major axes of the elliptical cross section, the orthogonal direction being the a axis. We identified in previous experiments[17] that the elastic constant C_{33} showed the strongest anomalies at the SP transition. It is obtained by measuring the velocity of ultrasonic longitudinal waves propagating along the c axis. This velocity is measured with a pulsed acoustic interferometer yielding a sensitivity in velocity variation better than 1 ppm. The longitudinal waves are generated at 30 MHz and odd overtones by 36° Y-cut coaxially plated $LiNbO_3$ piezoelectric transducers bonded to the crystal faces with GE Silicon Sealant. In this frequency range the ultrasonic velocity is not dependent on frequency: all the data reported in this paper were obtained around 100 MHz. Parallel faces perpendicular to the appro-

 © 1997 The American Physical Society

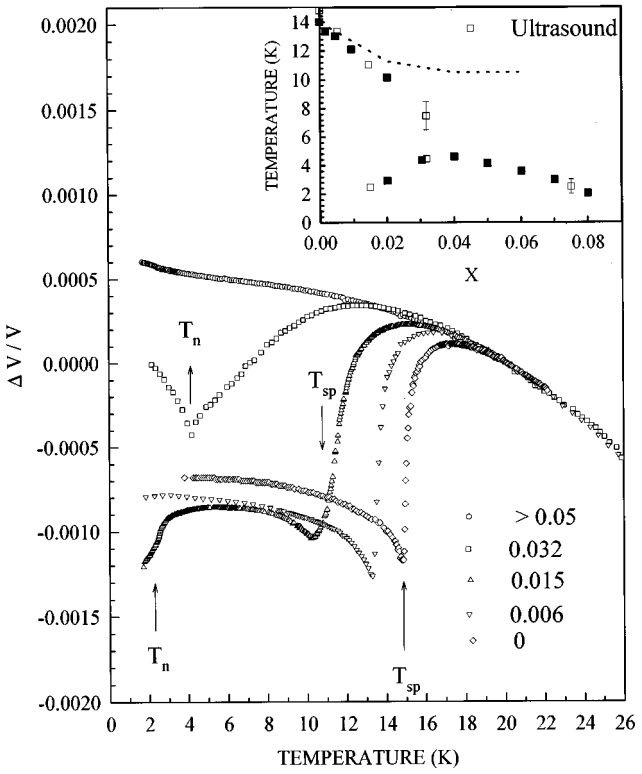

FIG. 1. Relative variation of the ultrasonic velocity as a function of temperature for $Cu_{1-x}Zn_xGeO_3$ single crystals. T_{SP} and T_n indicate, respectively, the SP and AF transition temperatures. Inset: Concentration phase diagram: susceptibility (black squares) from Ref. 1, neutron scattering (dotted line) from Ref. 4.

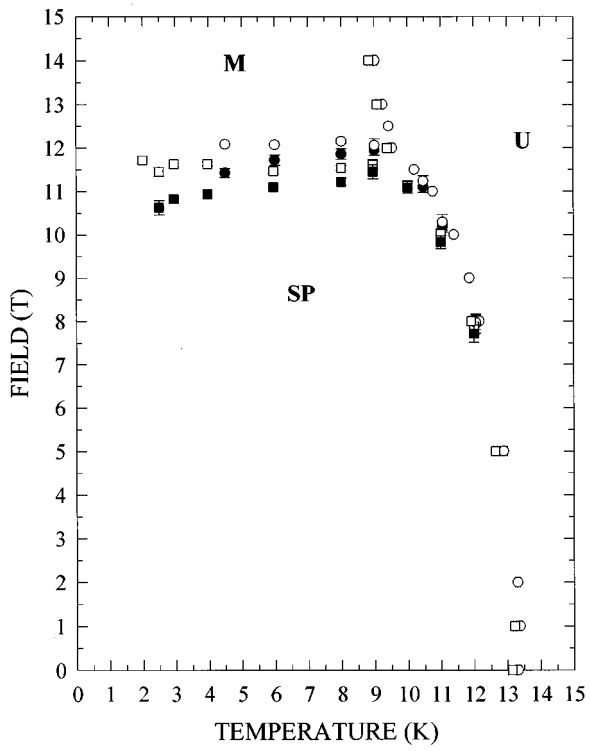

FIG. 2. Magnetic phase diagram for $Cu_{0.994}Zn_{0.006}GeO_3$: $H||c$ (circle) and $H||a$ (square); white and black for increasing and decreasing field, respectively.

priate propagation direction are obtained after delicate polishing of the crystal with diamond paste. Propagation lengths around 5 mm are typically used in each experiment. The crystal is mounted at the end of a calorimeter head which can be oriented easily in the magnetic field supplied by a 14 T superconducting magnet. Helium exchange gas is used for sample thermalization. The temperature is monitored and stabilized with a LakeShore Controller and two sensors: a capacitance sensor for magnetic field measurements is calibrated with a Si diode in zero field.

III. RESULTS

The elastic constant C_{33} has an anomalous temperature dependence between 20 and 300 K due to an important magnetoelastic coupling between the magnetic chains and the phonons.[18] This anomalous character is not a precursor of the SP transition since it is found in heavily doped (Si, Zn) crystals for which the transition is absent.[19] Above 20 K the ultrasonic velocity is identical for all the studied Zn-doped crystals. Differences are only observed in the vicinity of the magnetic transitions below 20 K as it can be seen in Fig. 1 where the relative variation of the velocity is shown. In the pure crystal, as reported in Ref. 8, the velocity softens from 22 K down to $T_{SP}=14.5$ K where an abrupt decrease is observed. In these ultrasonic experiments T_{SP} is defined as the temperature where the variation of the velocity is the largest (maximum slope indicated by arrows in Fig. 1). Below T_{SP} the velocity stiffens with a temperature dependence typical of an order parameter. For the $x=0.006$ crystal the velocity softens at lower temperature and T_{SP} is shifted down to 13.5 K; the abrupt decrease at T_{SP} is somewhat larger than in the pure crystal but the stiffening at lower temperature is the same. A very weak slope variation of the velocity is observed below 3 K in agreement with the growth of an AF state. For higher concentrations the overall temperature dependence of the velocity is modified. For $x=0.015$, in addition to the softening occurring at lower temperatures, the decrease at T_{SP} is less abrupt and somewhat smeared: T_{SP} is shifted to 11 K and the amplitude of the decrease is smaller. A stiffening is again seen below 10 K but a further softening takes place at lower temperature where another magnetic transition occurs at T_N (defined as the maximum slope variation). For a higher concentration (0.032), the smearing of the SP transition is so important that it is difficult to define a clear transition temperature. If we use the inflection point of the curve shown in Fig. 1, we evaluate $T_{SP}=7.5\pm1.0$ K. On the other hand, the AF transition is well established at 4.4 K. For $x>0.05$ (but less than 0.1 which is the nominal value), the SP transition has disappeared: a small stiffening at $T=2.5\pm0.5$ K, probably a remnant of a magnetic transition, is observed. In the inset of Fig. 1 we plotted the values obtained for T_{SP} and T_N as function of the concentration x. We added for comparison susceptibility[1] and neutron-diffraction[4] data: the agreement is excellent. The SP state seems to be maintained up to high concentrations and the magnetic transition observed at T_N is associated with an AF Néel state. This will be discussed now more thoroughly.

For each crystal the magnetic phase diagram is obtained by following the anomalies observed in the velocity for field sweeps at fixed temperature and temperature sweeps at fixed

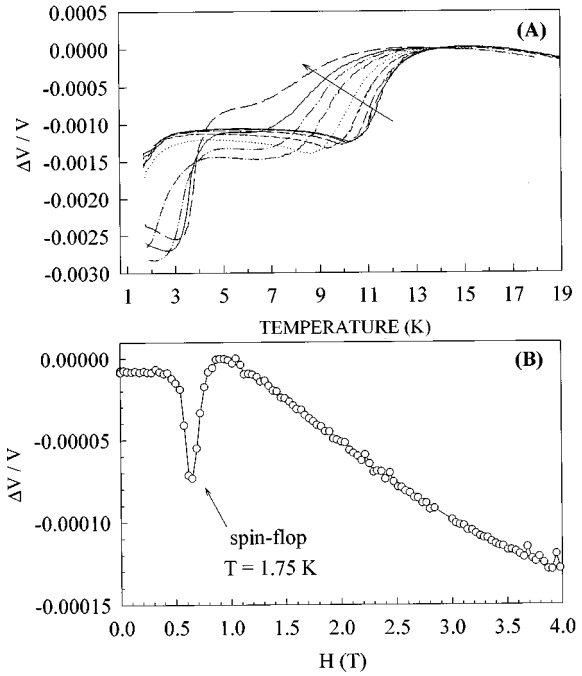

FIG. 3. Relative variation of the ultrasonic velocity for $Cu_{0.985}Zn_{0.015}xGeO_3$: (a) temperature sweeps at fixed magnetic field: 0, 2, 4, 6, 8, 10, 11, 12, and 14 T (the arrow indicates the increasing field); (b) field sweep at $T=1.75$ K.

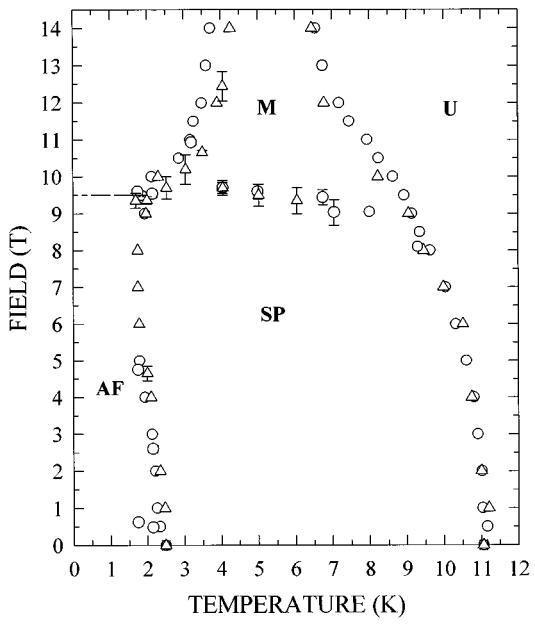

FIG. 4. Magnetic phase diagram for $Cu_{0.985}Zn_{0.015}GeO_3$: $H||c$ (circle) and $H||a$ (triangle). The dashed line is an extrapolation of the SP-M line.

field. For fields oriented along the a and b axes, the phase diagrams are practically identical, the location of the phase boundaries differing only according to the relevant g factor. Only data obtained along the c and a axes (the chain axis being c) will thus be presented in the following. The phase diagram for the $x=0.006$ crystal is presented in Fig. 2. It has all the characteristics of a typical SP phase diagram. Three boundaries separating the three phases, the dimerized (SP), the magnetic (M), and the uniform (U) phases, are identified. Compared to the pure crystal,[20] the SP-M line is located at a lower field (just below 12 T) and it represents a first-order transition since a subtantial hysteresis is observed (the other transition lines are second order). As the critical point is approached, the transition becomes progressively of second order. The main effect of light doping of $CuGeO_3$ by Zn is thus a reduction of the temperature and field scales over which the SP state is observed. As indicated in Fig. 1, a small anomaly in the velocity occurs below 3 K in zero field; this anomaly is modified by the magnetic field when it is oriented along the c axis. These results were not added to the phase diagram because the anomaly is not well characterized. We believe however that this reveals the growth of an AF state.

We present in Fig. 3(a) the relative velocity variation as a function of temperature at fixed field values (oriented along the c axis) for the $x=0.015$ crystal. It is clear from this figure that the elastic anomalies are highly modified by a magnetic field and a different magnetic phase diagram should be expected. The diagram is shown in Fig. 4. For $T>4$ K the lines of a typical SP phase diagram are identified. We believe that the SP-M line centered at 9.5 T extends below 2 K as indicated by the dashed line; this will be discussed later. Moreover, other boundary lines are observed below 4 K. For the field oriented along the c axis, a horizontal line centered just over 0.5 T is added. This transition is shown in Fig. 3(b) where a field sweep at 1.75 K reveals a sharp peak around 0.6 T. Such a dependence is typical of a spin-flop (SF) transition:[8] the spins are aligned preferentially along the c axis in zero field and at H_{SF} they flop along a perpendicular direction. For this crystal the temperature range over which the SF transition is observed being too small, we will postpone a more complete characterization to the study of the next crystal.

When $x=0.032$ the SP transition can only be identified through the velocity softening below 12 K and a slight slope variation around 7 K when the AF Néel transition gives rise to a clear anomaly just above 4 K as indicated in Fig. 1. We doubt that the softening below 12 K can be related to AF fluctuations since the temperature range over which they extend is too large (4–12 K) compared to the Néel temperature. Because the SP transition is not clear enough for this crystal, we will present only the low temperature phase diagram. The velocity variation as a function of temperature at fixed field (oriented along the c axis) is presented in Fig. 5. The shape of the anomaly is not modified very much as the magnetic field is varied from 0 to 14 T. This means that the nature of the AF state is maintained over the magnetic field range. The phase diagram is shown in Fig. 6. For both field orientations the AF-SP(?) boundary is a vertical line up to 8 T: for higher field values the critical temperature increases weakly up to 14 T. For $H||c$, the vertical line is shifted down by 0.3 K because a spin-flop (SF) transition occurs around 1 T. The inset of Fig. 6 shows the critical point region. This diagram is consistent with an easy axis along the chain direction (c axis). The angular dependence of the SF field, H_{SF}, is shown in Fig. 7. When the field is moved away from the easy axis, H_{SF} grows easily to 2.5 T for an angle of 40° along the b direction but it stays pinned to 1 T up to 25° along the a direction. This behavior also observed for the

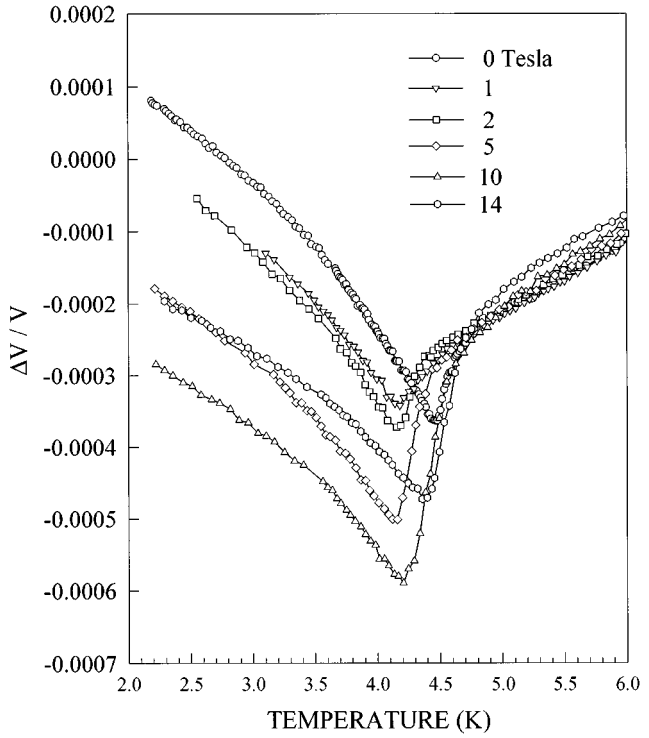

FIG. 5. Relative variation of the ultrasonic velocity for $Cu_{0.968}Zn_{0.032}GeO_3$. Temperature sweeps are at fixed magnetic field.

$CuGe_{0.993}Si_{0.007}O_3$ crystal[8] is consistent with orthorhomic anisotropy as determined by Hase *et al.*:[13] easy axis along c, intermediary axis along a, and hard axis along b.

The last crystal with $x>0.05$ shows also an anomalous

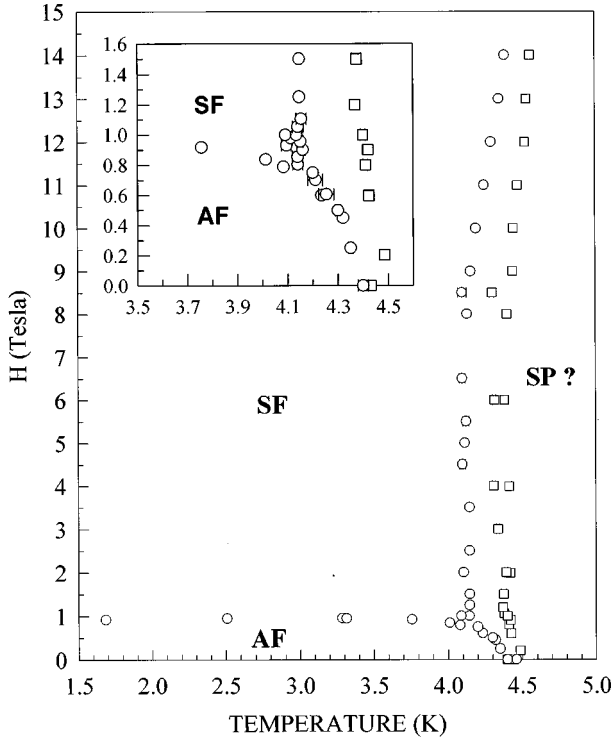

FIG. 6. Magnetic phase diagram for $Cu_{0.968}Zn_{0.032}GeO_3$: $H||c$ (circle) and $H||a$ (square). Inset: critical point region.

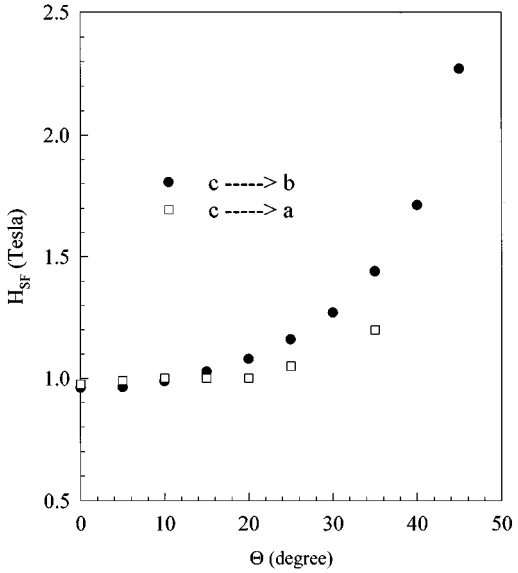

FIG. 7. Angular dependence of the spin-flop field H_{SF} for $Cu_{0.968}Zn_{0.032}GeO_3$.

behavior below 19 K. In Fig. 8 we compare the temperature dependence of the velocity variation at 0 and 14 T. The velocity being practically field independent above 12 T, the 14 T curve represents a reference curve which is free of magnetic transition effects. From this figure it is thus possible to assert that a magnetic transition is occurring around 2.5 K where a stiffening is observed; this value of T_N yields a concentration x around 0.075 (smaller than the nominal value 0.1 as expected) according to the inset shown in Fig. 1. At higher temperatures the softening is likely related to SP fluctuations since they are observed up to 17 K, a temperature too high to be associated to the magnetic transition.

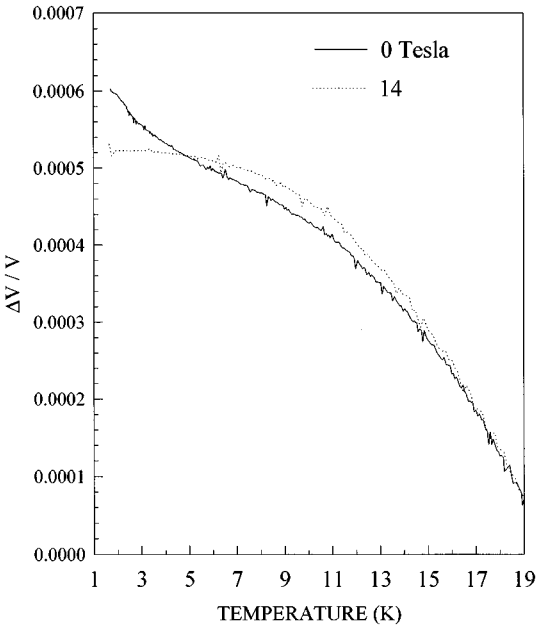

FIG. 8. Relative variation of the ultrasonic velocity for $Cu_{1-x}Zn_xGeO_3$, x $>$ 0.05. Temperature sweeps at fixed magnetic field.

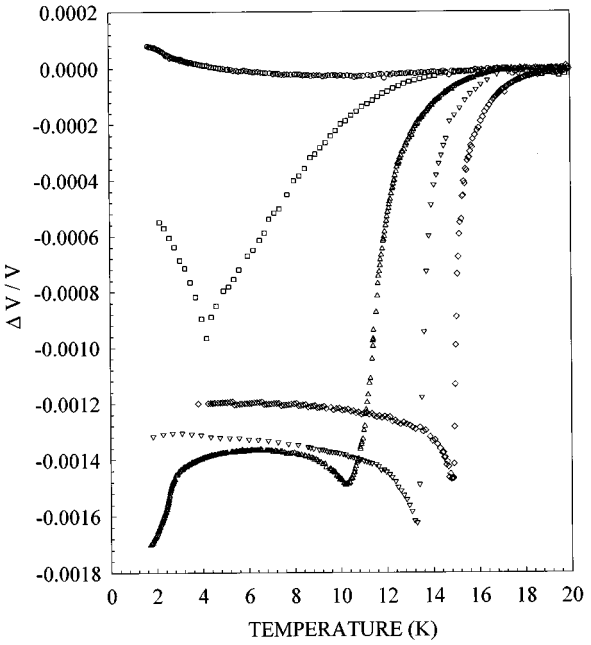

FIG. 9. Magnetoelastic contribution to relative variation of the ultrasonic velocity for $Cu_{1-x}Zn_xGeO_3$ as a function of temperature. Symbols are defined in Fig. 1.

IV. DISCUSSION

The ultrasonic velocity data presented in the preceding section are particularly revealing to understand the effects of doping in the SP compound $CuGeO_3$. The growing of a long-ranged AF Néel state is clearly established for intermediate concentrations together with the progressive shift of the SP transition to lower temperatures. In Fig. 9 we show the relative softening of the velocity due only to the magnetic transitions: these data were obtained from Fig. 1 by subtracting the normal elastic behavior given by the 14 T curve ($x>0.05$) of Fig. 8. For each crystal, the substantial softening observed below 20 K is indicative of pretransitional SP fluctuations. A clear SP transition, in the thermodynamic sense, occurs only for $x<0.032$. According to x-ray diffuse scattering experiments,[12] the 3D long-range SP modulation is suppressed for a fraction of a percent of Si or Zn substituent. We thus believe that the temperature dependence of the elastic anomaly below T_{SP} and the smearing of the transition as x is increased are consistent with a short-range-ordered state in Zn-doped crystals. Among these compounds, $x=0.032$ seems to constitute a limiting value of the concentration where a transition to an ordered SP state (short-range) ceases to occur. For this value of x, the temperature range over which the pretransitional fluctuations are observed extends down to T_N where the long-range AF state appears. This is in contrast with the neutron scattering data of Sasago *et al.*[4] who suggest that the SP state in 2% and 4% Zn-doped crystals is long range in nature with a T_{SP} around 10 K.

Before examining the question of the coexistence of the SP and AF states in these crystals, it is worthwhile to compare the doping effects of Si and Zn. The magnetic phase diagram of a $CuGe_{0.993}Si_{0.007}O_3$ crystal has been obtained previously with the same ultrasonic technique.[8] When compared to the diagram of $Cu_{0.994}Zn_{0.006}GeO_3$ (Fig. 2), it seems clear that doping effects are stronger in Si-doped crystals: the AF state is established at a lower concentration and the shift in T_{SP} is larger. For this Si-doped crystal, the boundary line between the M phase and the AF and/or SP phases is clearly observed. Moreover the AF part of the diagram is very similar to the diagram shown in Fig. 6 for the $x=0.032$ concentration. It thus seems likely that the diagram of $CuGe_{0.993}Si_{0.007}O_3$ is constructed from a superposition of two different diagrams: one is the typical SP diagram whose example is given in Fig. 2 for the $x=0.006$ Zn crystal, the other being the AF Néel diagram of Fig. 6. A different superposition of these diagrams is observed in Fig. 4 for the $x=0.015$ Zn crystal: the abrupt slope variation of the AF-SP vertical line indicates the crossing of the SP-M line centered at 9.5 T and extending below 2 K. This extension of the SP-M line below 2 K is a sensible assumption, although it has not been experimentally determined since lower temperatures could not be attained with our ultrasonic setup. In Fig. 6 the vertical boundary line presents also a change of slope (absent for the Si-doped crystal since the AF-SP line merges with the M-U line) at 8 T: we believe that this is an additional indication of the presence of the SP state.

The magnetic phase diagrams of Zn-doped $CuGeO_3$ crystals are consistent with a coexistence of the SP and AF states as it has been suggested in neutron-diffraction experiments.[4,9] They are also consistent with a limitation of the SP order (short-range) for both types of doping with an enhancement for the Si compounds as previously suggested by Schoeffel *et al.*[12] There is however a question that still has to be answered: can a macroscopic phase separation explain the coexistence of these two ordered states? Although the homogeneity and the Zn content were scrutinized, we did not check the crystals for a possible phase separation since such an analysis is difficult to perform because of the very low Zn content. On the other hand, if such a separation had occurred, our grown crystals would have been of a poorer quality than the one obtained, which is comparable to the pure $CuGeO_3$. Finally, if we examine carefully the AF part of the various diagrams, the change of curvature of the vertical line around 9 T (Fig. 4) suggests a coupling between the two ordered states: a phase separation is thus unlikely.

V. CONCLUSION

We reported in this paper that Zn doping limits the SP order in $CuGeO_3$ in a more severe way than Si. From an observation of the magnetic phase diagrams of Zn-doped crystals with different concentrations we observed that, although an AF Néel state with orthorhombic anisotropy has clearly settled over a wide concentration range, a limited SP order is definitely established and coexists with the AF state. This assumption is consistent with the presence of SP fluctuations in all studied crystals and with the fact that the magnetic phase diagram looks like a mere superposition of AF and SP diagrams. These results are in excellent agreement with neutron-diffraction experiments.

ACKNOWLEDGMENTS

The authors acknowledge the technical assistance of Mario Castonguay and fruitful discussions with Benoit

Dumoulin, Guy Quirion, and Martin Plumer. They are also grateful to Jean Beerens for giving access to his 14 T experimental setup. This work was supported by grants from the Fonds pour la Formation de Chercheurs et l'Aide à la Recherche of the Government of Québec (FCAR), from the Natural Science and Engineering Research Council of Canada (NSERC), and NEDO (Japan).

[1] M. Hase, I. Terasaki, Y. Sasago, K. Uchinokura, and H. Obara, Phys. Rev. Lett. **71**, 4059 (1993).
[2] M. Hase, N. Koide, K. Manabe, Y. Sasago, K. Uchinokura, and A. Sawa, Physica B **215**, 164 (1995).
[3] M. Hase, K. Uchinokura, R.J. Birgeneau, K. Hirota, and G. Shirane, J. Phys. Soc. Jpn. **65**, 1392 (1996).
[4] Y. Sasago, N. Koide, K. Uchinokura, M.C. Martin, M. Hase, K. Hirota, and G. Shirane, Phys. Rev. B **54**, R6835 (1996).
[5] S.B. Oseroff, S.-W. Cheong, B. Aktas, M.F. Hundley, Z. Fisk, and L.W. Rupp, Jr., Phys. Rev. Lett. **74**, 1450 (1995).
[6] J.G. Lussier, S.M. Coad, D.F. McMorrow, and D. McPaul, J. Phys. Condens. Matter **7**, L325 (1995).
[7] J.-P. Renard, K. Le Dang, P. Veillet, G. Dhalenne, A. Revcolevschi, and L.-P. Regnault, Europhys. Lett. **30**, 475 (1995).
[8] M. Poirier, R. Beaudry, M. Castonguay, M.L. Plumer, G. Quirion, F.S. Razavi, A. Revcolevschi, and G. Dhalenne, Phys. Rev. B **52**, R6971 (1995).
[9] L.P. Regnault, J.P. Renard, G. Dhalenne, and A. Revcolevschi, Europhys. Lett. **32**, 579 (1995).
[10] S. Inagaki and H. Fukuyama, J. Phys. Soc. Jpn. **52**, 2504 (1983); **52**, 3620 (1983).
[11] H. Fukuyama, T. Tanimoto, and M. Saito, J. Phys. Soc. Jpn. **65**, 1182 (1996).
[12] J.P. Schoeffel, J.P. Pouget, G. Dhalenne, and A. Revcolevschi, Phys. Rev. B **53**, 14 971 (1996).
[13] M. Hase, M. Hagiwara, and K. Katsumata, Phys. Rev. B **54**, R3722 (1996).
[14] A. Revcolevschi and R. Collongues, C.R. Acad. Sci. **266**, 1767 (1969).
[15] A. Revcolevschi, Rev. Int. Hautes Temp. **7**, 73 (1970).
[16] J.C. Rouchaud, N. Boisseau, and M. Fedoroff, J. Radioanal. Nucl. Chem. Lett. **175**, 25 (1995).
[17] M. Poirier, M. Castonguay, A. Revcolevschi, and G. Dhalenne, Phys. Rev. B **52**, 16 058 (1995).
[18] B. Dumoulin, P. Fronzes, M. Poirier, A. Revcolevschi, and G. Dhalenne, Synth. Met. (to be published).
[19] S. Jandl, M. Poirier, M. Castonguay, P. Fronzes, J.K. Musfeldt, A. Revcolevschi, and G. Dhalenne, Phys. Rev. B **54**, 7318 (1996).
[20] M. Poirier, M. Castonguay, A. Revcolevschi, and G. Dhalenne, Phys. Rev. B **51**, 6147 (1995).